2022 IEEE 5th International Conference on Soft Robotics (RoboSoft)
April 4-8, 2022, Edinburgh, UK

Design of a Robotic Foot with Midtarsal Joint Locking Mechanism

Kazuma Enomoto[1], Tsung-Yuan Chen[1], Takumi Kawasetsu[1], and Koh Hosoda[1]

***Abstract*— Understanding the intrinsic softness of the human foot and implementing its essential functions in a biped robot could improve walking performance. In this study, we propose a design of a robotic foot with bioinspired midtarsal joint locking mechanism. The proposed foot has joints to form the arch of the human foot, and the stiffness of the foot can be changed by the locking mechanism. To investigate the dynamic behavior of the mechanism during walking, we conducted experiments on the proposed foot with different locking angles. We evaluated the results by comparing the ground reaction forces and propulsive forces. The proposed foot was mounted on a walking simulator to reproduce a single walking step. We confirmed two peaks in the ground reaction force, as observed in humans. We found differences in the second peak, which was caused by the midtarsal joint locking mechanism. A difference in the generated propulsive force was confirmed from the locking angle of the midtarsal joint. The results of this study could facilitate designing a robotic foot that utilizes its adjustable softness to realize walking in a biped robot.**

***Index Terms*— Soft Robot Applications, Humanoid and Bipedal Locomotion, Biologically-Inspired Robots, Robotic Foot, Midtarsal joint**

I. Introduction

Humans walk by skillfully utilizing musculoskeletal structures, and the human foot is a notable example of this. It is a strong body support composed of a complex structure. This structure contains 26 bones, 33 joints, and more than hundred muscles, tendons, and ligaments. In contrast, most of the existing biped robots are equipped with rigid and flat feet. One of the reasons for this could be restriction owing to mathematical models and control methods, such as zero moment point or inverted pendulum model [1], [2]. However, these simple feet lack the softness of the human foot structures and cannot easily handle external disturbances during stable walking. Therefore, understanding the functions of the softness of the human foot structure during walking may allow improving the walking performance of biped robots [3], [4], [5], [6].

The complex structure of the foot produces numerous essential functions for stable walking. Among these functions, the stiffness change of the foot contributes to the body support, transmission of the kicking force to the ground, and shock absorption at different times during walking[7], [8]. These functions appropriately adjust the ground reaction force (GRF) during bipedal walking [5], [9].

In the foot structure, the locking mechanism of the midtarsal joint contributes to the change in the stiffness the foot [10]. An anatomical experiment suggested that when the foot touches the ground, the motions of the talus and calcaneus reduces the mobility of the midtarsal joint. The locking mechanism can be considered as a function to brake the rotation of the midtarsal joint at a certain time, that is, a certain angle of the midtarsal joint [10]. This function can be reproduced by a simple rotation axis that reproduces the midtarsal joint and a locking mechanism of the rotation axis [11]. Nevertheless, little is known about the contribution of the angle of the stiffness change by the midtarsal joint locking mechanism to the GRF and propulsive force. This is because conducting quantitative and comparative experiments with/without a foot structure using conventional approaches such as cadavers and human experiments is difficult.

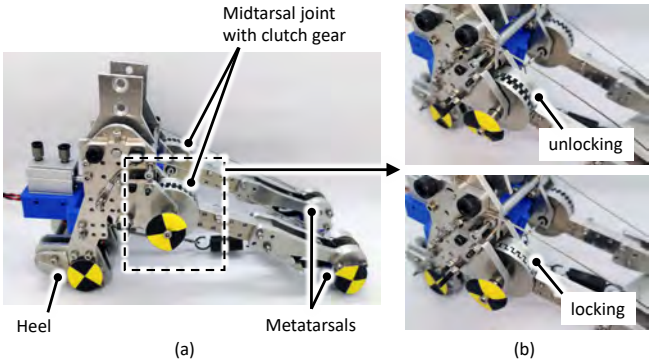

Fig. 1. Picture of the proposed robotic foot using the midtarsal joint locking mechanism. The midtarsal joint is located at the apex of the instep and is equipped with clutch gears for the locking mechanism. The stiffness of the foot can be controlled by engaging the clutch gear.

In this study, we investigated the relationship between the locking angle of the midtarsal joint and changes in GRF and propulsive force.

Herein, we propose a bioinspired robotic foot with a locking mechanism of the midtarsal joint based on an anatomical functional study (see Fig. 1). This foot has a single rotation joint that simplifies the midtarsal joint. We attached a clutch gear to the joint to brake and lock the rotation of the midtarsal joint. Using these designs, the proposed foot has two states: soft and rigid states. I the former, the midtarsal joint can rotate freely, whereas in the latter, the rotation is locked. To investigate the contributions of the developed robotic foot to the GRF, a stepping experiment was conducted using a dynamic walking simulator.

The structure of this paper is as follows: Section II introduces the proposed robotic foot, and describes the experimental procedure. Section III evaluates the performance of

This work was supported in part by JSPS KAKENHI under Grant JP18H05467.

[1] Graduate School of Engineering Science, Osaka University, Osaka 5600044, Japan. enomoto.kazuma@arl.sys.es.osaka-u.ac.jp

2022 IEEE 5th International Conference on Soft Robotics (RoboSoft) | 978-1-6654-0828-8/22/$31.00 ©2022 IEEE | DOI: 10.1109/ROBOSOFT54090.2022.9762172

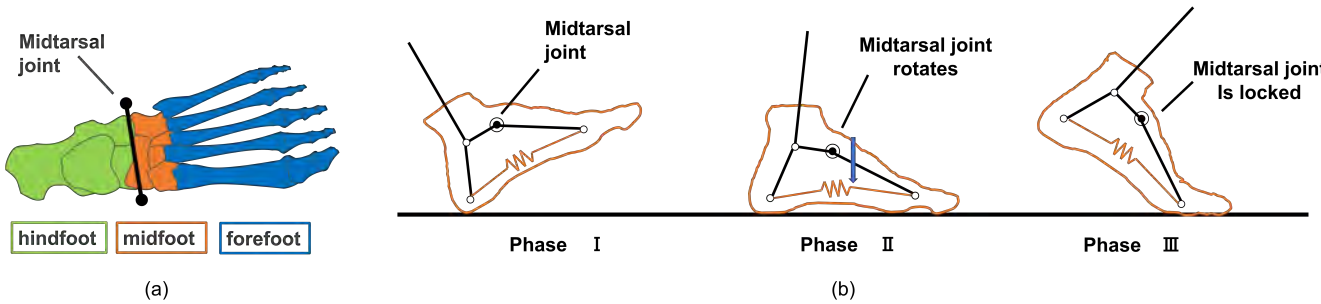

Fig. 2. Structure and function of the human foot: (a) The bone of the human foot structure viewed from above. Anatomically, the green, orange, and blue parts represent hind foot, mid foot, and forefoot, respectively. The black axis running through the red part is the midtarsal joint. (b) Phase classification according to the contact part of the foot with the ground during walking. In Phase I, the heel contacts the ground first and the body is supported by the heel alone. In Phase II, the toe contacts the ground and thus the body is supported by the whole foot. The softness generated by the rotation of the midtarsal joint and the deformation of the arch absorb the shock of foot landing. In Phase III, the heel leaves the ground and the body is supported by the toes alone. The midtarsal joint locking mechanism works and the forefoot acts as a lever to kick the ground.

the developed foot during stepping and investigates its effect on the simulator. Section IV discusses the experimental results. Section V presents the conclusions and future research prospects of this study.

II. Methods

A. Structure and function of the human foot

The human foot can be divided into three parts: the forefoot, midfoot, and hindfoot (see Fig. 2 (a)). The midtarsal joint is located between the hindfoot and midfoot as shown by the black solid line. In clinical studies, it is also known as Chopart's joint. Some studies have reported that the softness of the forefoot and midfoot changes depending on the deformation state of the hindfoot [10], [12]. One example is the midtarsal joint locking mechanism [10]. The forefoot supports the body and generates propulsive forces when the foot kicks the ground [4]. The forefoot and hindfoot are connected by the plantar fascia. The combination of these three parts may properly regulate the foot stiffness during walking.

As shown in Fig. 2 (b), the human gait is briefly divided into three phases according to the literature [9], [12]. In phase I, only the heel touches the ground, which is also known as the initial contact phase. In phase II, both the heel and forefoot touch the ground, also known as the midstance phase. In phase III, the heel leaves from the ground, and the body is supported only by the forefoot. This phase is also called the propulsion phase. In the above gait phases, the locking mechanism of the midtarsal joint plays an essential role in stiffness control [13], [14].

B. Robotic foot design

Figures 1 and 3 illustrate the structure and working principle of the proposed robotic foot. The dimensions of the developed foot are 240 mm in length, 58 mm in heel width, 92 mm in forefoot width, and 72 mm in height of the midtarsal joint, in reference to the human foot [15]. The body and the foot are connected at the hindfoot. The midtarsal joint was designed as a parallel axis to allow the foot to rotate around the pitch axis. This joint connects the hindfoot and both the first and fifth metatarsals. Each metatarsal can rotate around the joint axis independently. As illustrated in Fig. 3 (a), the tip of each metatarsal and the heel are connected by a wire and a spring (k=2.16 N/mm) as the plantar fascia.A microswitch was attached to the bottom of the heel to detect the ground contact timing of the foot.

To change the stiffness of the midtarsal joint, we designed a joint locking mechanism to lock the rotation of the joint using a pair of custom clutch gears. The clutch gear was fabricated by machining with aluminum. The diameter of the gear was 40 mm, and it had 30 rectangular-shaped teeth on the circumference (see also Fig. 3 (b) upper). A pneumatic cylinder was used to pull the gear attached to the hindfoot (clutch gear 1) to engage the other gear attached to the metatarsal (clutch gear 2) as shown in Fig.3 (b). Clutch gear 1 was fixed to the hindfoot to prevent its rotation against the hindfoot. Thus, the joint movement of the midtarsal joint was locked by engaging the gears. A conical spring was inserted between the two gears to passively disengage the gears when the cylinder is released. In this design, the locking angle of the midtarsal joint can be determined by adjusting the teeth placement angle of the clutch gear.

C. Experimental environment and procedures

In this study, we used a dynamic walking simulator to reproduce a single step in a human walk [16]. Figure 4 shows the experimental environment. The simulator had three legs (fore, middle, and hind legs), and the developed robotic foot was attached to the middle leg. A weight of 10 kg was installed at the top of the simulator to apply a load to the foot. In addition, we attached a weight of 2.5 kg to the simulator through a wire to pull it toward the x-axis direction. With these settings, the simulator's average walking speed was 0.9 m/s, and we could conduct the experiment without it tipping over sideways.

The experimental procedure is illustrated in Fig. 5. In the initial position, only the hind leg touched the ground, and the simulator was fixed using an electromagnet. When the electromagnet was released, the simulator was pulled by the weight toward the x-axis direction. The heel of the

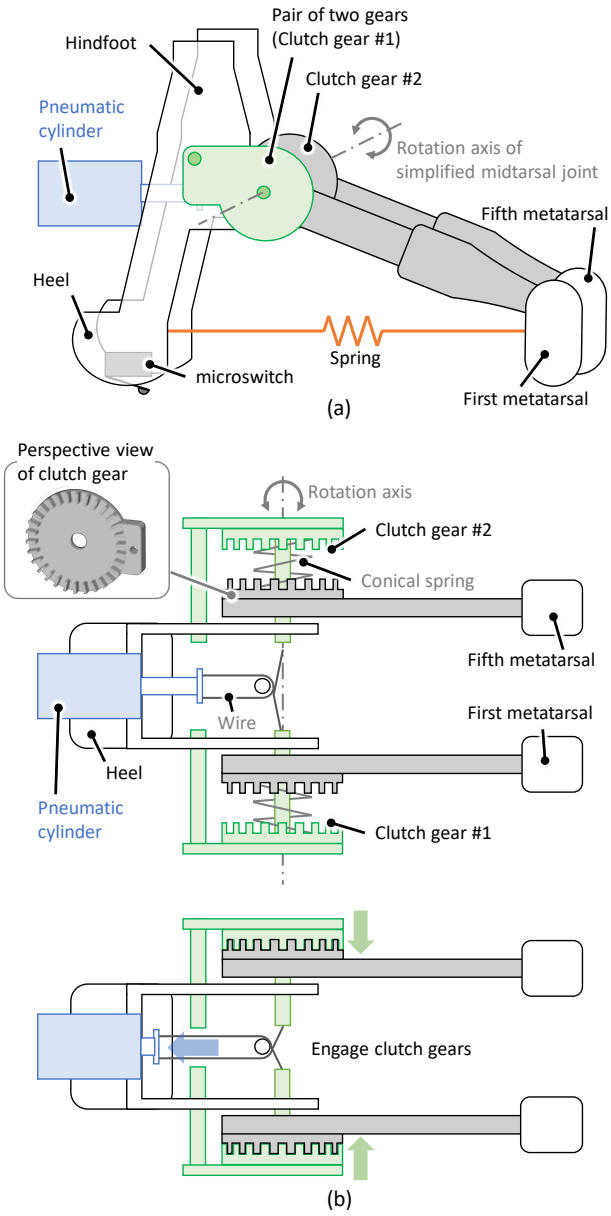

Fig. 3. Structure and working principle of the joint locking mechanism of the proposed foot: (a) Perspective and (b) top views of the foot. Engaging the clutch gears attached to the midtarsal joint locks its joint movement. Upper and bottom of the figure (b) correspond to the unlock and lock states of the midtarsal joint, respectively.

robotic foot contacted the ground, and the hind leg left the ground (phase I). The toes of the robotic foot then touched the ground. Thus, the entire foot supported the load of the simulator (phase II). Thereafter, the heel of the foot left the ground, and only the toe supported the simulator (phase III). In phase III, the toe also kicked the ground, thereby generating a propulsive force along the x-axis. Finally, the fore leg of the simulator touched the ground, and the toe of the foot left the ground (final position).

We designed five comparative conditions, as shown in Table I, to investigate the relationship between the locking angle, GRF, and propulsive force. Herein, we define the angle

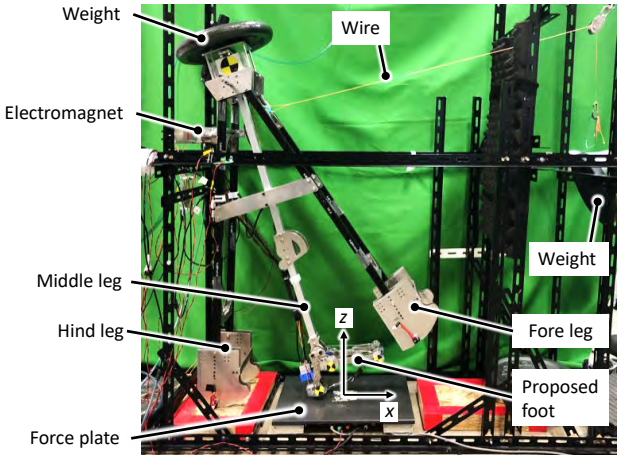

Fig. 4. Illustration of the experimental environment. The proposed foot was installed to the middle leg of a dynamic walking simulator. We installed a force plate to measure the GRF and propulsive force produced by a single step.

TABLE I

FIVE-LOCKING ANGLE CONDITIONS OF THE MIDTARSAL JOINT.

condition	θ (degree)
Fixed	0
Lock 1	6
Lock 2	12
Lock 3	18
Free	Not defined

θ as the inclination of the middle leg from the vertical upward direction (see Phase III on Fig. 5). The angle θ is controlled by adjusting the time between the heel contact detected by the microswitch and the clutch gear engagement. The Lock 2 condition locks the rotation of the midtarsal joint at an angle closest to that of typical human walking [17]. The Lock 1 and Lock 3 conditions lock the rotation of the joint at smaller and larger angles compared to that of a human, respectively. In the free condition, the rotation of the joint does not lock in all phases. In contrast, the fixed condition keeps the joint locked in all phases.

The GRF was measured using a force place (TF-4060, Tec Gihan Co., Ltd, Japan). The sampling frequency of the force plate was 1 kHz. During phase III, the propulsive force was also evaluated by calculating the power product, that is, the integral of the measured force along the x-axis, F_x over time. All kinematic data were filtered using a fourth-order low-pass Butterworth filter with a cut-off frequency of 14 Hz. Statistical tests were conducted using one-way ANOVA with Tukey's post honestly significant difference (HSD) tests.

III. RESULTS

The results of GRF and propulsive force measurements with respect to time are presented in Fig. 6. Ten trials were conducted to test different experimental conditions. The results were organized according to the phases described earlier.

From the results of GRF measurements, we confirmed that the GRF exhibited 1) a peak at phase I (first peak) under

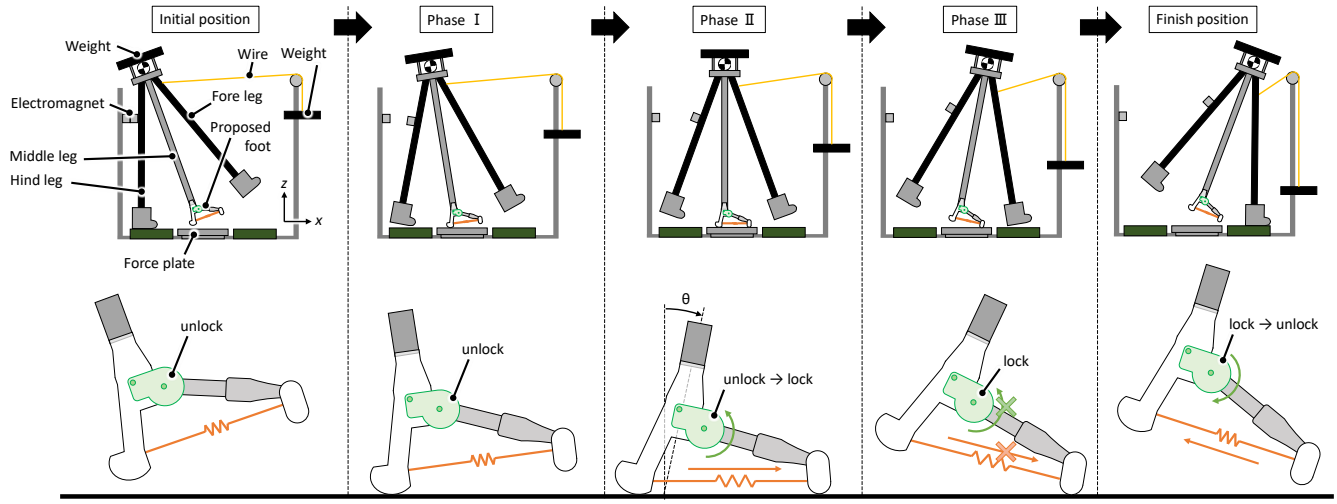

Fig. 5. Walking procedure and its phases. First, the heel of the foot touches the ground (phase I). Then, the tip of the foot touches the ground, and the clutch gear is engaged when the midtarsal joint rotate to an angle θ (phase II). The heel of the foot leaves the ground (phase III), and finally the whole foot leaves the ground (finish position). The lock and unlock represent the locking and unlocking state of the locking mechanism, respectively.

all conditions, and 2) a peak in phase III (second peak) under Lock 1, Lock 2, Lock 3 and Fixed conditions. The results of propulsive measurements suggested tha a positive force was generated in phase I under all conditions. In contrast, significant positive and negative propulsive forces were generated in phase III.

We compared the relationship between the locking angle of the midtarsal joint and the GRF in phase III under all conditions, except for the Free condition. Figure 7 shows the average peak values of the GRF in phase III. The results can be summarized as follows: 1) Significant differences were observed under each condition, except under the Lock 1 and Fixed conditions. 2) The peak value in phase III of the GRF was smaller in the Lock 3 condition than in other conditions, while those in other conditions were similar.

We evaluated changes in the propulsive force under all conditions, except the free condition. Figure 8 shows the power product of the propulsive force in phase III averaged over 10 trials. The results demonstrated that 1) significant differences were observed under each condition, except between the Lock 3 and Fixed conditions, 2) the amount of the propulsive force in the Lock 2 condition was the largest in all conditions, and 3) the amount of the propulsive force was small under the Lock 3 and Fixed conditions. We also found that the propulsive force in the Lock 2 condition was approximately twice as large as that in the Lock 1 condition.

IV. Discussion

This study evaluated the contribution of the midtarsal joint locking mechanism of the human foot to ground reaction force generation by constructing a bioinspired robotic foot. We confirmed that the proposed locking mechanism enabled the locking of the midtarsal joint rotation at an arbitrary locking angle.

The results of the GRF measurements revealed that the Free condition had no tendency of increasing the GRF in phase III (Fig. 6 (e)). This is because the foot does not have a rigid state, that is, the midtarsal joint can rotate freely among all the walking phases; thus, the foot cannot effectively kick the ground. In contrast, the GRFs in phase III increased under other conditions (Fig. 6 (a)–(d)). Moreover, under these conditions, the robotic foot became rigid, that is, the midtarsal joint was locked before the foot left the ground. The peak values observed under different locking conditions in phase III indicate generation of largest and smallest GRFs under Lock 2 and 3 conditions, respectively (Fig. 7). The above findings suggest that the rigidity of the foot plays an important role in GRF generation during ground kicking, and that the locking angle may affect the GRF generation.

The GRF generation when the foot kicked the ground in phase III also contributed to propulsive force generation during walking. In this study, we compared the propulsive force generation by evaluating the power product of the force along the x-axis in phase III. The results show that the propulsive force was large under the Lock 2 condition, while the force was significantly small under the Lock 3 and Fixed conditions. These results suggest that the locking angles adjust the propulsive force generation.

Considering an ideal bioinspired robotic foot design, an adjusting mechanism that can switch between rigidity and softness of the foot is an essential function in stable walking [8]. Most of the existing studies on robotic feet have focused on adjusting the rigidity and softness of these feet by utilizing the properties of the plantar fascia [4], [5], [9]. In contrast, this study proposed a bioinspired mechanism that enables switching of the rigidity and softness of the foot by directly controlling the locking status of the midtarsal joint. The proposed mechanism provides a example of a bioinspired robotic foot.

Anatomical studies suggested that the midtarsal joint can be considered an oblique joint [18]. However, here we designed the midtarsal joint by simply rotating the pitch

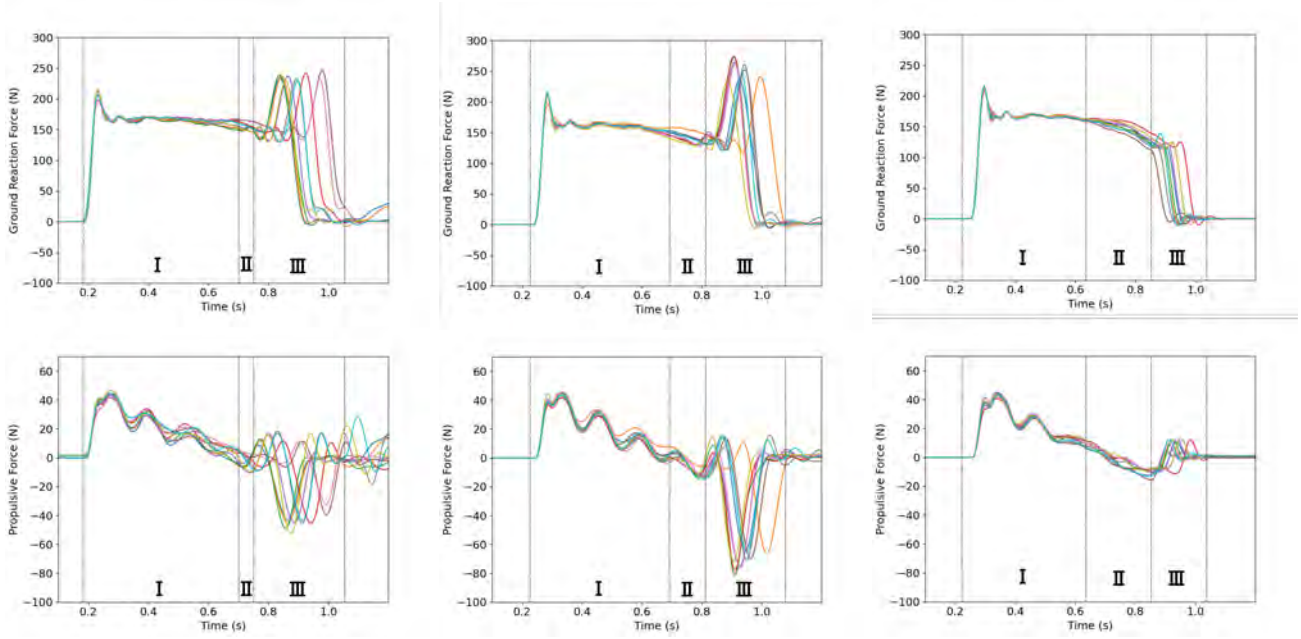

(a) Lock 1 (b) Lock 2 (c) Lock 3

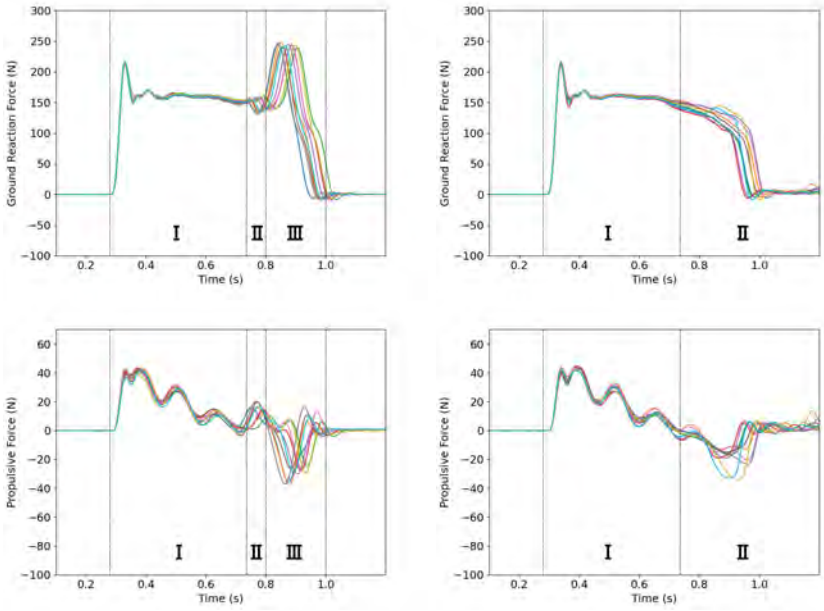

(d) Fixed (e) Free

Fig. 6. Results of GRF and propulsive force measurements over time. (a) Lock 1 condition: The lock angle of the midtarsal joint θ 6 $^\circ$; (b) Lock 2 condition: θ 12 $^\circ$; (c) Lock 3 condition: θ was 18 $^\circ$; (d) Fixed condition: θ was 0 $^\circ$; and (e) Free condition. The numerals I, II, and III denote phase I, phase II, and phase III, respectively, during walking.

axis. The oblique midtarsal joint contributes to the generation of a vertical yaw moment at the supporting foot [5]. Yaw moment generation is also an important function for realizing stable walking. Therefore, for future work, we will focus on understanding the contribution of the combination of the oblique joint and the proposed locking mechanism.

V. Conclusion

We proposed a robotic foot with a midtarsal joint locking mechanism, and investigated the relationship between its locking angle and both the GRF and propulsion force. The experimental results demonstrated that the GRF and propulsive force were maximum under the condition where the locking angle was close to that of the human midtarsal joint. Moreover, the values of these forces decrease at other

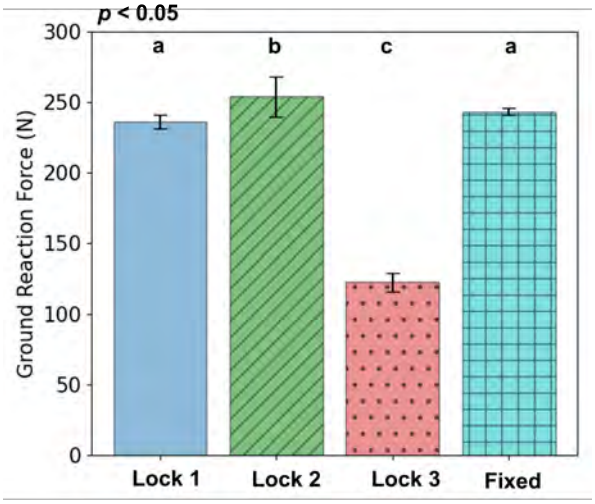

Fig. 7. Comparison of the peak values of GRF in phase III under different locking conditions. The bar and error bar (mean s.d.) indicate the average and standard deviation of GRF over 10 trials, respectively. Groups sharing the same letter are not significantly different by using the visualization method of the general statistic [19].

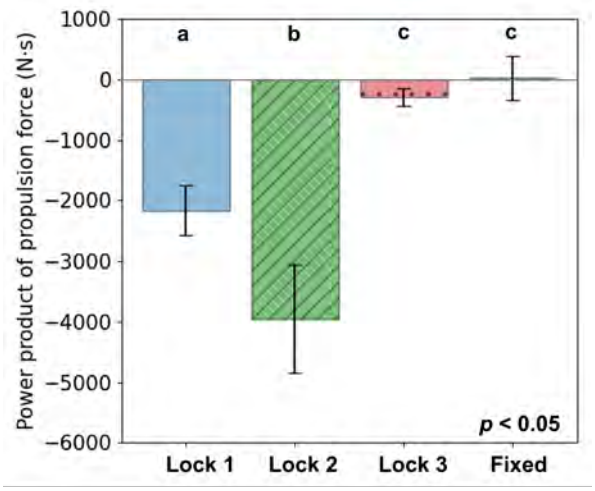

Fig. 8. Comparison of the power product of propulsion force in phase III under different locking condition. The bar and error bar (mean s.d.) indicate the average and standard deviation of force product over 10 trials, respectively. Groups sharing the same letter are not significantly different by using the visualization method of the general statistic [19].

four locking angles. The results of this study could facilitate designing a robotic foot that utilizes its adjustable softness to realize efficient walking in a biped robot.

Because the proposed robotic foot can arbitrarily adjust the locking angle of the midtarsal joint, the foot can potentially adjust its stiffness to enhance the walking performance even under complicated terrain. For future work, we will investigate the relationship between walking performance, GRF, and propulsive force under various environments to obtain the appropriate locking angle.

REFERENCES

[1] M. Vukobratović and B. Branislav, "Zero-moment point—thirty five years of its life," Intl. J. Humanoid Robotics, vol.1, no.1, pp.157–173, 2004.
[2] S. Kajita, et al., "The 3D linear inverted pendulum mode: A simple modeling for a biped walking pattern generation," Proc. 2001 IEEE/RSJ Intl. Conf. Intelligent Robots Syst., Expanding the Societal Role of Robotics in the Next Millennium, vol.1, pp.239–246, 2001.
[3] C. Piazza, et al., "Toward an adaptive foot for natural walking," 2016 IEEE-RAS 16th Intl. Conf. on Humanoid Robots (Humanoids), pp.1204–1210, 2016.
[4] X. Liu, et al., "Using the foot windlass mechanism for jumping higher: a study on bipedal robot jumping," Robot. and Auton. Syst., vol.110, pp.85–91, 2018.
[5] T. Chen, et al., "Free moment induced by oblique transverse tarsal joint: investigation by constructive approach," R. Soc. Open Sci. vol.8, no.4, pp.201947, 2021.
[6] H. Seki, T. Nagura, Y. Suda, N. Ogihara, K. Ito, Y. Niki, M. Matsumoto, and M. Nakamura, "Quantification of vertical free moment induced by the human foot-ankle complex during axial loading," Proc Inst Mech Eng H., vol.232, no.6, pp.637–640, 2018.
[7] J. Perry, and J. M. Burnfield, "Gait analysis. Normal and pathological function 2nd ed," SLACK Incorporated Publishing, Thorofare, NJ, 2010.
[8] D. Torricelli, et al., "Human-like compliant locomotion: state of the art of robotic implementations," Bioinspir. biomim., vol.11, no. 5, p.051002, 2016.
[9] K. Narioka, T. Homma, and K. Hosoda, "Humanlike ankle-foot complex for a biped robot," Proc 2012 IEEE-RAS Intl. Conf. Humanoid Robots (Humanoids), 2012.
[10] C. B. Blackwood, T. J. Yuen, B. J. Sangeorzan, and W. R. Ledoux, "The midtarsal joint locking mechanism," Foot Ankle Intl., vol.26, no.12, pp.1074–1080, 2005.
[11] Hicks, J. H. "The mechanics of the foot: I. The joints." Anat., vol. 87, no. Pt 4, pp.345, (1953).
[12] Hashimoto, Kenji, et al. "A study of function of foot's medial longitudinal arch using biped humanoid robot." 2010 IEEE/RSJ Intl. Conf. Intellg. Robots and Systems. IEEE, 2010.
[13] N. Okita, et al. "Midtarsal joint locking: new perspectives on an old paradigm," J. Orthop. Res., vol.32, no.1, pp.110–115, 2014.
[14] P. Caravaggi, et al., "A dynamic model of the windlass mechanism of the foot: evidence for early stance phase preloading of the plantar aponeurosis," J. Exp. Biol., vol.212, no.15, pp.2491–2499, 2009.
[15] Y. Lee, et al., "Comparing 3d foot shape models between taiwanese and japanese females," J. Human Ergo., Vol.44, No.1, pp. 11–20, 2015.
[16] Ito, Kohta, et al. "Direct assessment of foot kinematics during human gait using a dynamic cadaver simulator and a biplane X-ray fluoroscopy." J. Foot Ankle Res. vol. 7. no. 1, 2014.
[17] Ito, Kohta, et al. "Three-dimensional innate mobility of the human foot bones under axial loading using biplane X-ray fluoroscopy." R. Soc. Open Sci, vol.4, no.10, pp.171086, (2017).
[18] J. L. Tweed, et al, "The function of the midtarsal joint: a review of the literature," The Foot, vol.18, no.2, pp.106–112, 2008.
[19] Yamada, Mayu, et al. "Multisensory-motor integration in olfactory navigation of silkmoth, Bombyx mori, using virtual reality system." Elife no.10, pp.e72001, (2021).